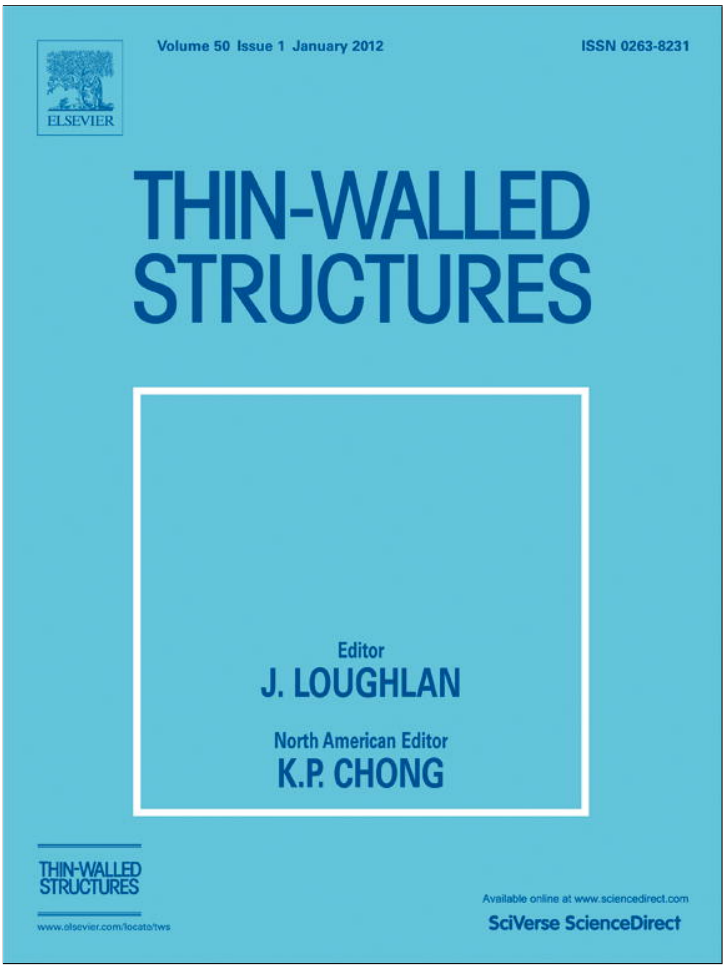

(This is a sample cover image for this issue. The actual cover is not yet available at this time.)

Thin-Walled Structures 54 (2012) 35–43

Contents lists available at SciVerse ScienceDirect

Thin-Walled Structures

journal homepage: www.elsevier.com/locate/tws

Instability of cylindrical shells with single and multiple cracks under axial compression

Babak Haghpanah Jahromi, Ashkan Vaziri *

Department of Mechanical and Industrial Engineering, Northeastern University, Boston, MA 02115, USA

ARTICLE INFO

Article history:
Received 31 October 2011
Received in revised form
10 January 2012
Accepted 25 January 2012

Keywords:
Cracked cylinder
Eigenvalue analysis
Buckling behavior
Finite element model

ABSTRACT

Linear eigenvalue buckling analysis was carried out for singly and doubly cracked cylindrical thin shells under axial compression using the finite element method. First, the effect of crack size and orientation on the buckling behavior of an axially loaded shell with a single crack was studied. Then, the buckling behavior of a cylinder with two parallel longitudinal cracks was investigated. Two different buckling shapes with cross-sectional deformation profiles that resemble letters M (symmetric) and N (anti-symmetric) were identified as the first buckling modes of the cylinder. The exchange between these local buckling modes due to variation of crack size and spacing was illustrated. The transition between these two buckling shapes can be used to estimate the 'maximum interaction distance' of the cylinder cracks—the separation distance beyond which the two cracks do not interact in affecting the buckling load of the cylindrical shell. The influence of shell thickness and crack length on the maximum interaction distance was quantified for cylinders with two co-centered (i.e., parallel offset) or collinear longitudinal cracks. Additional simulations were carried out for cylinders with multiple symmetrically spaced longitudinal cracks to show how the behavior of single and double cracks can give the buckling load and mode shape of cylinders with multiple cracks.

1. Introduction

Defects can have a significant influence on the behavior of thin-walled structures. From the structural point of view, the most detrimental consequence of a defect is the excessive stress, which could result in fracture at or near the defect location and possibly overall structural failure. Defects could also lead to large localized deformations (e.g. local buckling or plastic deformation), which can alter the structure's load carrying capacity or function [1–5]. Thus, there is a driving need to better understand the effect of defects on the mechanical behavior and structural performance of plates and shells. We have chosen to focus on cracks, which could appear due to overload, fatigue, manufacturing errors, or harsh environmental condition. The mechanics of cracked shells have been studied extensively in recent decades. These studies range from development of theoretical approaches to better understand stress distribution and structural behavior of the shell in the presence of defects [6–15], and numerical simulations of linear and nonlinear response of cracked shells under loading [16–28], to experimental investigation of shells with defects [29–37].

Cracked shells have often been explored numerically, since this makes it possible to probe the response over a broad range of geometrical parameters and loading conditions. However, most of these studies are focused on investigating the role of a single defect (e.g., a crack) on shell failure. In this study, the role of single and multiple cracks on the eigenvalue buckling load of cylindrical shells – which represent the most common type of shells used in pipelines and marine or aerospace structures – was studied using finite element analysis. Finite element models of cracked cylinders were developed by extending a special plane stress crack tip meshing scheme developed by Estekanchi and Vafai [16] to the case of cylinders with multiple cracks. This approach accurately captures the crack-tip stress intensity factor with relatively few elements. The method has been previously used to study the eigenvalue buckling behavior of cracked plates [17,18] and cylinders with a single crack subjected to tension or compression [19,28], pure torsion [20] and combined axial compression and internal pressure [21]. This method simplifies the generation of numerical models of cracked shells and thus, allows comprehensive and parametric investigations on the behavior and mechanical response of cracked shells. More details of the computational models are provided in Section 2. In Section 3, we revisit the buckling of a cylinder with a single crack under axial compression which had previously been investigated by Estekanchi and Vafai [16] and Vaziri [19] for circumferential or

* Corresponding author.
E-mail address: vaziri@coe.neu.edu (A. Vaziri).

0263-8231/$ - see front matter © 2012 Published by Elsevier Ltd.
doi:10.1016/j.tws.2012.01.014

longitudinal crack orientations. Here, we expand those results by carrying out a parametric study for different crack orientations, and studying the appearance of non-symmetric mode shapes when cracks are not at 0° or 90°. In Section 4 we extend our study to cylindrical shells with two parallel cracks. For this purpose, we focused on parallel longitudinal cracks since the results in Section 3 show that a single longitudinal crack has the most detrimental effect on the buckling load of the cylindrical shell. We particularly studied the effect of crack separation distance. A maximum interaction distance, d_{im}, was defined as the separation beyond which the effect of any crack on the buckling load is decoupled from the effects of the other crack. In this case, the lowest buckling load of the cracked cylinder is dictated only by the worst-case crack, ignoring the others entirely. The dependence of the maximum interaction distance on cylinder thickness and crack size is exhibited for equal co-centered cracks (i.e., with parallel offset) and equal collinear cracks. In Section 5, we discussed how the results obtained for single- and double- cracked cylindrical shells could be used to understand the behavior of a cylindrical shell with multiple cracks. The conclusions were drawn in Section 6.

2. Finite element modeling of cracked shells

We used the meshing scheme proposed by Estekanchi and Vafai [16] for constructing the shell elements close to the crack tip. In this approach, the element size is relatively uniform everywhere away from the crack tips, while decreasing proportionally only in a region near the crack tip by approaching the crack tip. Fig. 1 shows an example of the developed finite element mesh based on this meshing scheme. The parametric study carried out in this work required constructing a substantial number of finite element computational models. We have developed a MATLAB code that allow automatic creation of the finite element model of cracked cylindrical shells with different crack length, a, and crack orientation, α, where $\alpha=0^\circ$ corresponds to circumferential direction. Furthermore, we developed an additional MATLAB code to create finite element models of cracked cylindrical shells with two parallel or collinear longitudinal cracks (i.e. both cracks having $\alpha=90^\circ$). Eight-node shell elements (S8R) with reduced integration and quadratic shape functions were used for the meshing. The cylindrical shell in the uncracked region was meshed into 150 elements in each of the axial and circumferential directions. For meshing the crack region, the zooming factor of 1/2 and zooming level of 6 were used. In this meshing scheme, the zooming level denotes the number of element layers surrounding the crack tip with reduced element size compared to uniform element size in the uncracked region, see Fig. 1. The zooming factor denotes the relative size (both length and width) of the element at each element layer to the size of the element in the previous element layer, as approaching the crack tip. This results in the crack tip element size 1/64 of the element size far from the crack tip. A sensitivity analysis was performed to assure that the obtained results are minimally sensitive to the selected mesh size.

Finite element models of cracked shells were numerically solved using Abaqus finite element package. The cylindrical shell was modeled as isotropic and linear elastic with Young's modulus $E=69$ GPa, and Poisson ratio $\nu=0.33$ (corresponding to the elastic properties of aluminum). Computational models of cracked cylindrical shells with length $l=2$ m, radius $R=0.2$ m, and various thickness t, were created. The cylinder shell was fully clamped at one end and was free to move in only the axial direction at the other end. The large l/R ratio adopted minimizes the effects of the end boundary conditions in the crack-containing mid-region of the cylinder [38]. A linear eigenvalue analysis was performed to obtain the buckling shape and buckling load of the cracked cylindrical shell. The calculated first mode buckling load of a cracked shell, F_c, was normalized by the theoretical buckling load of an uncracked cylinder with the same thickness, $F_t=3.8\ Et^2$, where E is the elastic modulus of the shell material [38]. The normalized buckling load of a cracked shell is denoted by $\gamma=F_c/F_t$.

3. Cylindrical shells with a single crack

A sufficiently short crack has no significant effect on the buckling behavior of a cylindrical shell: buckling occurs at $\gamma\sim1$ and covers the cylinder in axisymmetric corrugations with wavelength $2\pi*\sqrt[4]{R^2D/Et}$ where D is the flexural rigidity of the shell [38]. In contrast, a sufficiently long crack gives rise to buckling in the vicinity of the crack, with the buckling load $\gamma<1$. Figs. 2A and B show the normalized buckling load of a cylindrical shell with a single circumferential crack ($\alpha=0^\circ$) and a longitudinal crack ($\alpha=90^\circ$), respectively. The buckling loads were calculated using linear eigenvalue analysis for cracked cylinders with three different values of t/R, the shell thickness to radius ratio. The results show that a thinner cylinder suffers more from the presence of a given-length crack, and that in general a longitudinal crack has a

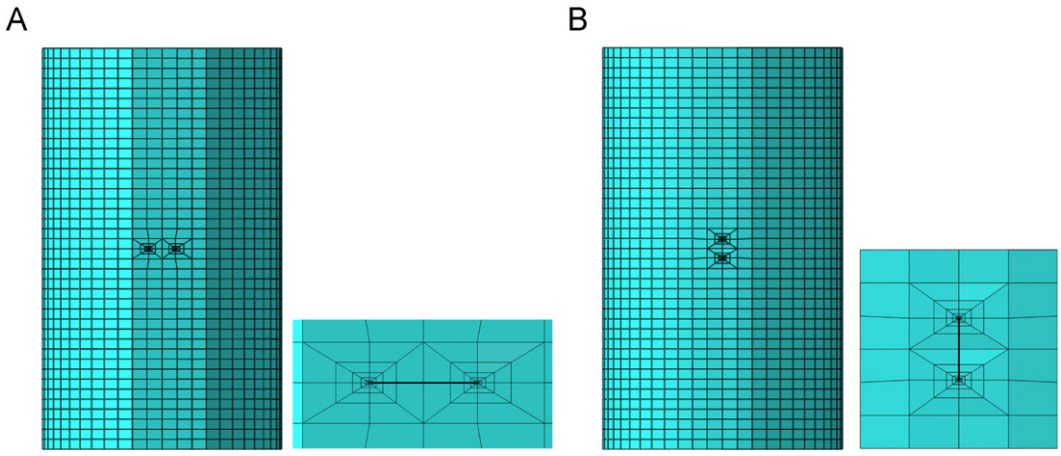

Fig. 1. Computational models of a cylindrical shell with (A) *a* circumferential crack and (B) an axial crack created by employing a special meshing scheme at the crack region proposed by Estekanchi and Vafai [16]. It should be noted that the actual mesh used in the finite element calculations was much finer than the mesh sizes shown in this figure.

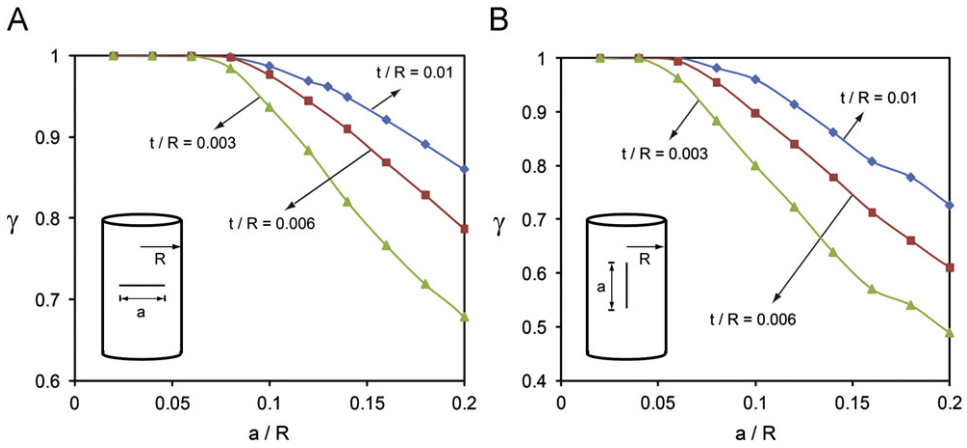

Fig. 2. Buckling of a single cracked cylindrical shell. γ, the buckling load normalized by that of an uncracked shell, versus crack length ratio, a/R, for cylindrical shells with (A) a circumferential crack ($\alpha=0^{\circ}$) and (B) an axial crack ($\alpha=90^{\circ}$). The results are presented for three thickness to radius ratios.

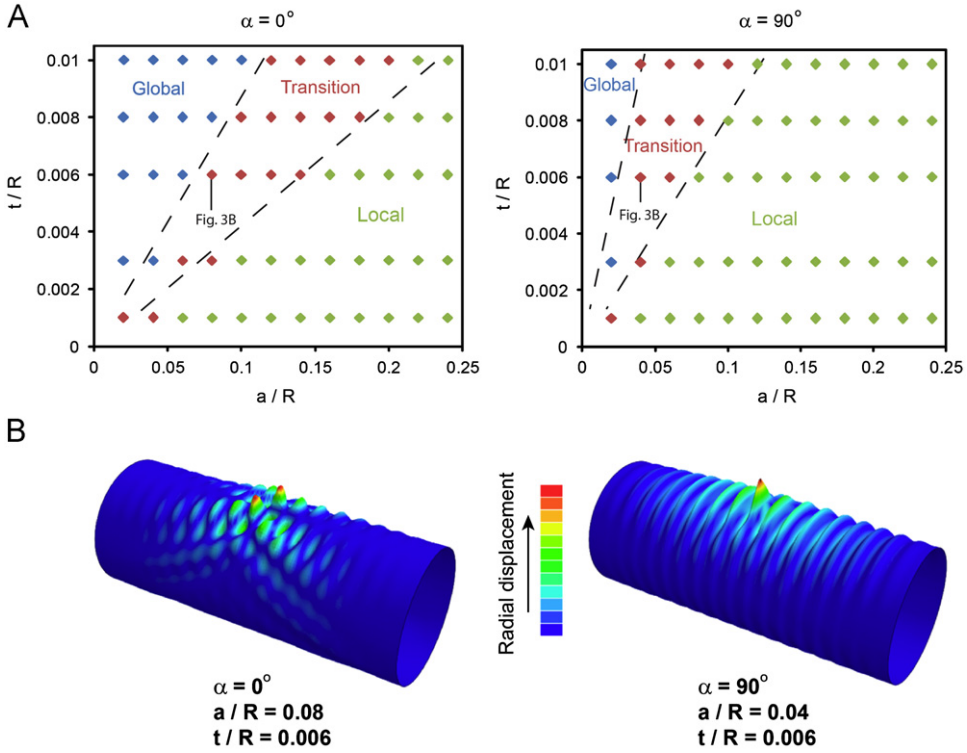

Fig. 3. (A) Global, transition and local buckling shapes for a circumferentially cracked (top left) and a longitudinally cracked (top right) cylindrical shell. (B) The transition buckling shape for the two cases identified in Fig. 3A.

more profound effect on cylinder buckling behavior compared to a circumferential crack. To study the transition from entire-cylinder to near-crack buckling as the crack length increases, we constructed buckling mode shape maps for cylinders with a circumferential or a longitudinal crack, Fig. 3 A. Three different distributions of buckling deformation were identified: (i) Global: The buckling shape and load are approximately the same as those of the counterpart uncracked cylinder (i.e. $0.95<\gamma<1$ with 'corrugations' distributed over the entire shell); (ii) Transition: The crack has an effect on both the buckling shape and the buckling load, but the buckling shape is not localized (the mode still involves most of the cylinder), see Fig. 3B. Depending on the thickness of the shell, a transitional buckling load of the cracked cylinder can be as low as 0.8 of the buckling load of the uncracked counterpart cylinder. (iii) Local: Buckling deformation is localized to the crack region, and the buckling load tends to be considerably lower than the buckling load of the counterpart uncracked shell. For the two studied crack orientations, the crack length associated with the transition between each two buckling shapes changes approximately linearly with the shell thickness, as shown by the dashed lines in Fig. 3A. Here, we define a critical crack length, a_c, as the maximum crack length leading to a truly global buckling shape as the first buckling shape of the cylinder. In this article, the critical crack length, a_c, is quantified as the crack length corresponding to the normalized buckling load equal to $\gamma=0.98$.

Fig. 4A shows the normalized buckling load of a cracked cylinder with $t/R=0.006$ as a function of crack length for different crack orientations, α. The buckling load of a cracked cylinder decreases as the crack changes from circumferential to longitudinal. In Fig. 4B, we have re-plotted the results to show the

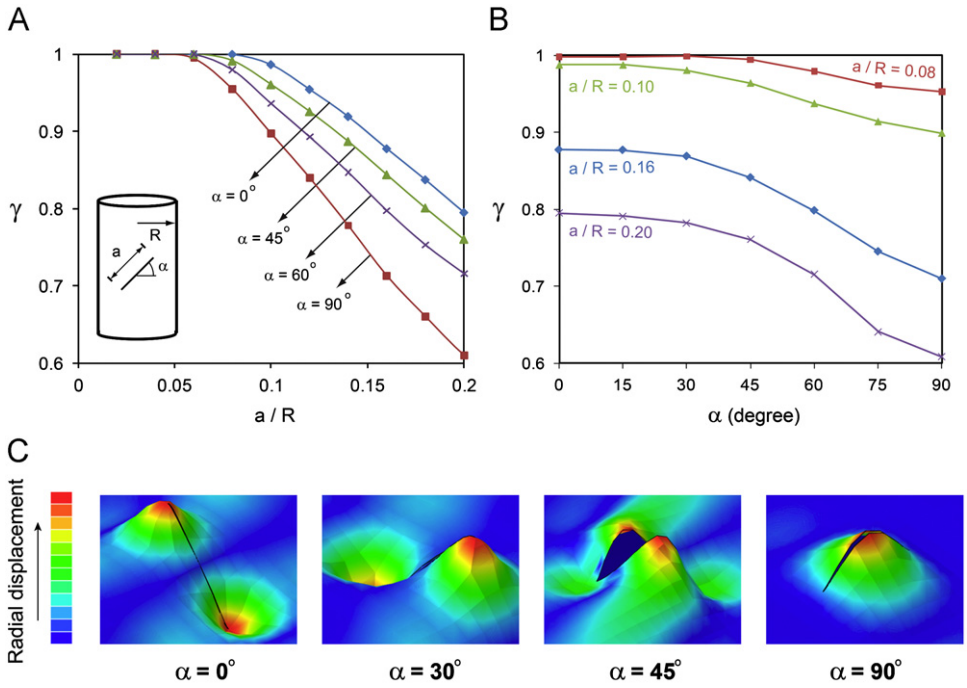

Fig. 4. (A) Normalized buckling load for a cylindrical shell with $t/R=0.006$ versus a/R for different crack angles, α. (B) Normalized buckling load for a cylindrical shell with $t/R=0.006$ versus the crack orientation. (C) Local buckling shapes for cracked-cylinders with different crack angles. Our analysis shows that the local buckling shape depends primarily on the crack angle, and is insensitive to the crack length and shell thickness.

cylinder buckling load versus the crack orientation for different crack lengths. The buckling load of a cracked shell with $\alpha < 30^\circ$ is approximately independent of the crack orientation. However, by further increasing the crack angle, the buckling load reduces significantly. Fig. 4C displays the buckling shapes of cylinders with four different crack angles. The local buckling mode shape is approximately independent of the cylinder thickness and the crack length. The cylinders with $\alpha=0^\circ$ and $\alpha=30^\circ$ have similar buckling shapes with maximum outward and inward displacements at the crack tips and the deformation is approximately symmetric with respect to the crack. The buckling shape of a cylinder with $\alpha=45^\circ$ is quite different, with the shell bulging out asymmetrically relative to the crack axis. In this case, the deformation at the crack tips is almost zero. The cracked cylinder with $\alpha=90^\circ$ bulges out symmetrically relative to the crack axis. In Fig. 5, we plotted the critical crack length (i.e. the length below which the 'global' buckling pattern predominates) normalized by cylinder radius, a_c/R, versus the crack orientation α, for three different cylinder thicknesses. The critical crack length changes nonlinearly with the crack orientation, α, and is higher for thicker cylindrical shells.

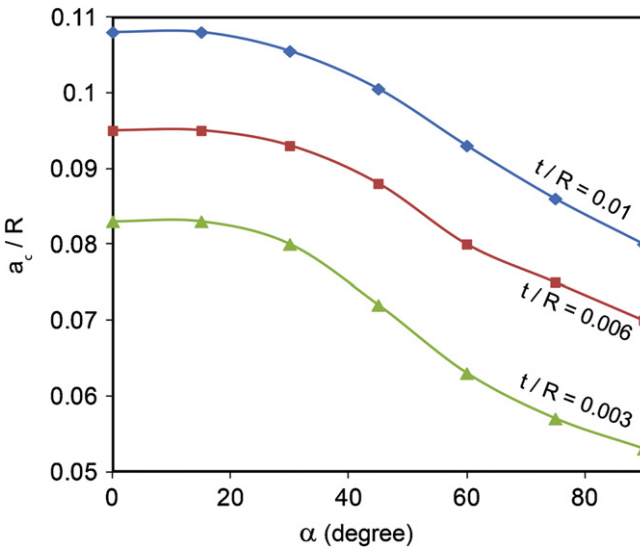

Fig. 5. Normalized critical crack length versus the crack angle for different shell thickness ratios, t/R. (The critical length is that below which a 'global' buckling mode becomes relevant.).

4. Cylindrical shells with two longitudinal cracks

In this section, we investigate the buckling behavior of a cylinder with two longitudinal cracks. The results provide insight into the elastic instability of shells with multiple parallel cracks, as will be discussed in Section 5. The choice of longitudinal cracks was made because, per unit length, this type of crack has the most detrimental effect on the buckling load of the cracked cylinder, as discussed in Section 3. As a starting point, we consider a cylindrical shell with two equal longitudinal cracks with length a located at distance d from each other in the circumferential direction, Fig. 6A. Fig. 6B shows the normalized buckling load of the cracked cylinder as a function of crack length for different crack separation distances. The buckling load of a cylinder with a single longitudinal crack is also shown for comparison. A cylinder with two parallel cracks, which are located relatively far from each other (e.g. $d/R=0.33$ in Fig. 6B), has a buckling load that is approximately equal to the buckling load of the same cylinder with a single longitudinal crack. In other words, once cracks are separated by more than the maximum interaction distance, they can be treated as isolated and the weakest (i.e. the one with the lowest buckling load) controls the load and appearance of buckling, The cylinder buckling load decreases somewhat when the distance between the two parallel cracks is reduced. The behavior at relatively small separation distance corresponds to buckling of the slender strip between two cracks.

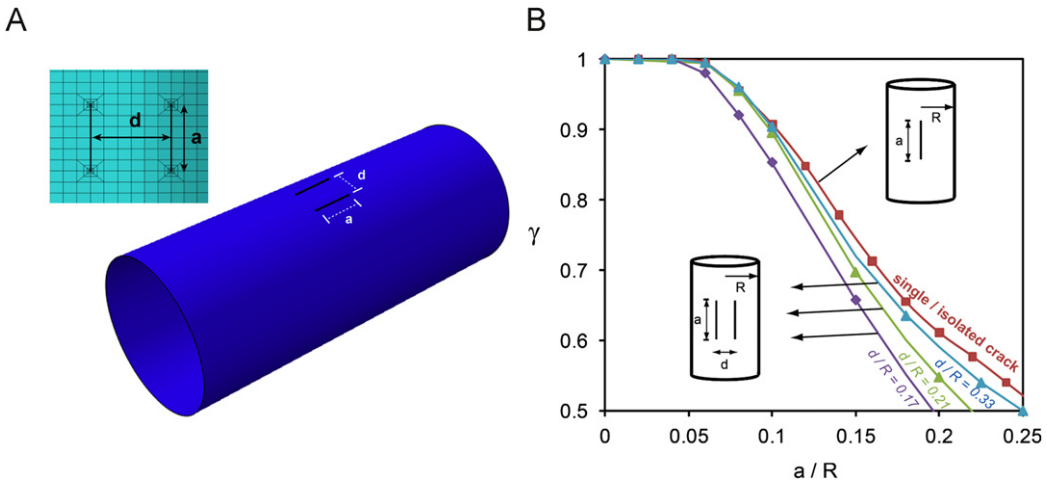

Fig. 6. Local buckling of a cylindrical shell with two, longitudinal, co-centered cracks. (A) Schematic of the cracked cylinder and the meshing scheme used for analysis. (B) Normalized buckling load of the cylinder versus the relative length of the two cracks, for a cylinder with $t/R=0.006$.

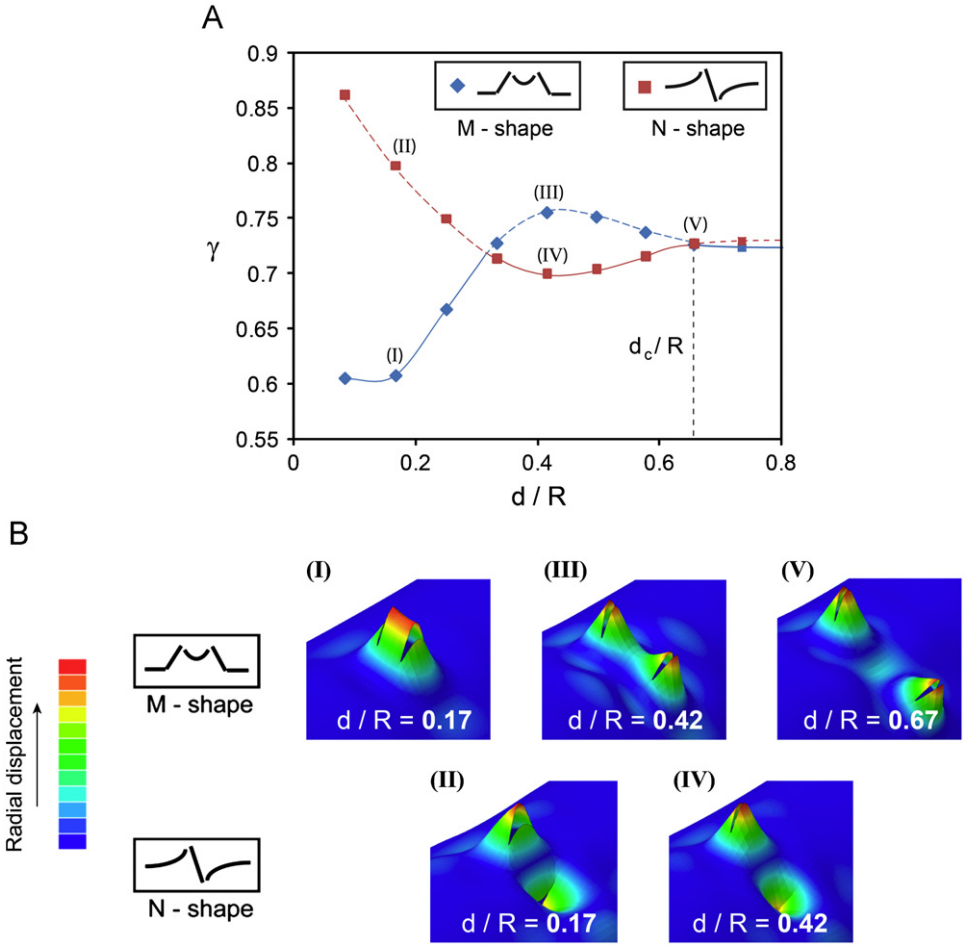

Fig. 7. (A) Normalized buckling load versus the relative separation distance of two cracks for a cylinder with $a/R=0.2$ and $t/R=0.01$. The solid line correspondes to the first (lowest load) mode of buckling, while the dashed line denotes the second mode. Red squares and blue diamonds correspond to the "M" (symmetric) and "N" (antisymmetric) shapes of buckling, which perform an exchange at $d/R=0.33$. (B) "M" and "N" shaped local buckling deformations for double-cracked cylinders of different crack separations, indicated in Fig. 7A. (For interpretation of the references to color in this figure legend, the reader is referred to the web version of this article.)

In order to better understand the interactions of adjacent cracks, we have studied the buckling mode shape as a function of parallel offset separation. Fig. 7 shows the buckling loads and mode shapes for the first two buckling modes of a cylindrical shell with $t/R=0.01$, $a/R=0.2$ versus different normalized crack distances, d/R. Two distinct buckling shapes are observed which are denoted as 'M' shape (symmetric) and 'N' shape (anti-symmetric). In the 'M' shape, the cylinder bulges locally outward at both cracks and the shell surface between the two parallel cracks moves outward with some symmetric bending. When the two cracks are located very close to each other (e.g. $d/R=0.17$, Case I in Fig. 7), the area between the two parallel cracks buckles like a

flat plate. For the 'N' shape, two local deformation peaks at the cracks' centers extend to opposite sides of the shell surface (i.e. outward and inward displacements). The surface between the two cracks deforms accordingly, as can be seen in cases II and IV. Half way between the two cracks there is a slope but no deflection. In Fig. 7B, we plotted the load associated with each mode as d/R is varied for the cylinder with $t/R=0.01$, $a/R=0.2$. For $d/R<0.35$, the lowest-load buckling mode of the cylinder is an 'M' shape, while for a larger value of d/R, an 'N' shape is the dominant (lowest load) mode of the cylinder buckling. An apparent discontinuity in lowest-mode shape is simply explained as a cross-over between these two modes with geometry-dependent eigenvalues. For $d/R>0.73$, the interaction of the two cracks is no longer significant and the buckling load is simply that of a cylinder with a single crack of the same size. In this case, the local mode consists of localized outward deformation of the crack edges, similar to the buckling shape of a longitudinally cracked shell—see Fig. 3C. The shell surface between the two parallel cracks has approximately zero deformation and zero slope. According to the above analysis, we defined a maximum interaction distance between two cracks, denoted by d_{im}, as the minimum distance at which the two cracks display an independent effect on the buckling behavior of the cylindrical shell. If the crack separation is greater than the maximum interaction distance, the buckling load of the cracked cylinder is determined purely by the larger crack alone. In this case the Section 3 results suffice for estimating the buckling mode shape and critical load based on the length of the larger crack. For the cylinder discussed in Fig. 7, the two cracks have the same size, $a/R=0.2$, and the normalized cylinder thickness is $t/R=0.01$. For this case, $d_{im}/R=0.73$.

For a given configuration (e.g. longitudinal co-centered cracks), the maximum interaction distance depends on the cylinder dimensions and crack sizes. In Fig. 8, we studied the buckling of a cylindrical shell with two longitudinal co-centered cracks of non-equal length. The length of two cracks were denoted by a and a_2, and the larger crack size was kept constant in the calculations and equal $a/R=0.2$. The size of the smaller crack was varied systematically $0\le a_2/a\le 1$, where $a_2/a=0$ corresponds a cylinder with a single crack of length a. Fig. 8B shows the dependence of the normalized maximum interaction distance, d_c/R, on a_2/a, for cylinders with three different thickness, $t/R=0.003$, 0.006 and 0.001. These results were obtained by performing a parametric study on the effect of crack distances on the buckling load and shape of the cylinder. For each case, this involves a set of calculations similar to the investigation discussed in Fig. 7. By increasing a_2/a, the maximum interaction distance increases nonlinearly. The maximum interaction distance is larger for thicker cylinders with the same crack size ratio, a_2/a, meaning that thick-cylinder results would be conservative compared to thinner cases. This outcome could perhaps be explained by the increase of the natural 'decay length' of a cylindrical shell which is proportional to $\sqrt[2]{R*t}$. The maximum interaction distance of the cracks also decreases as crack a_2 gets shorter, as quantified for selected cases in Fig. 8B. To further illustrate the effect of shell thickness on the maximum interaction distance of two equal size interacting cracks, in Fig. 8C we showed the normalized buckling load associated with the 'M' and 'N'-shaped interactional local buckling in cylinders with two cracks of equal length, $a/R=0.2$ and different thickness, $t/R=0.003$, 0.006 and 0.01.

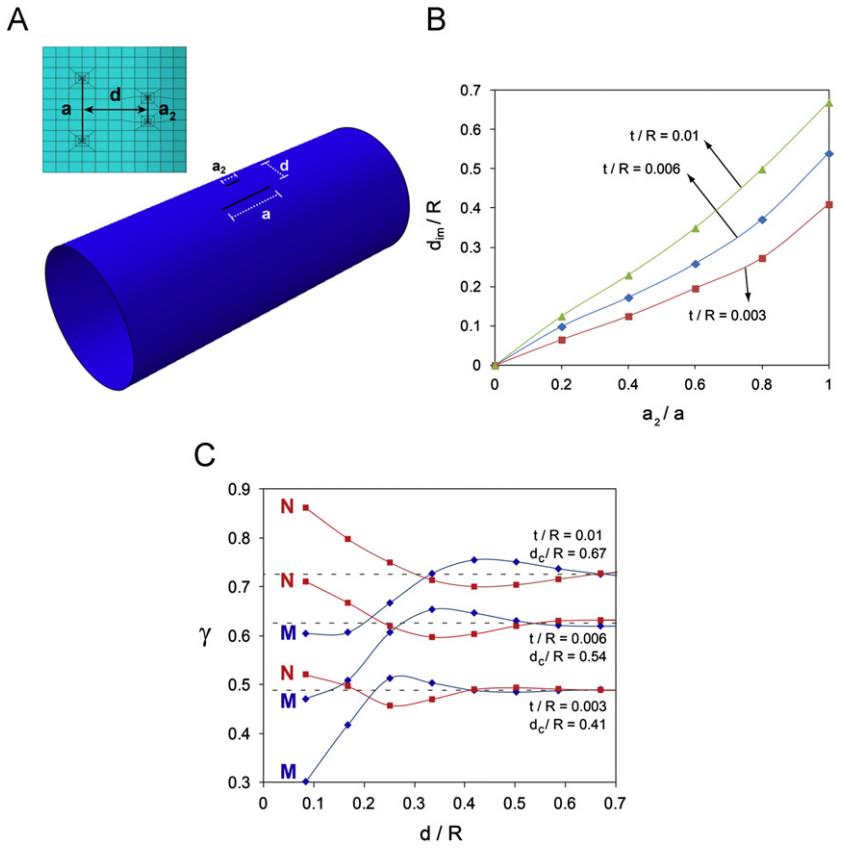

Fig. 8. Local buckling of a cylindrical shell with two different-size co-centered longitudinal cracks. (A) Schematic of the cracked cylinder and the meshing scheme used for analysis. (B) The maximum interaction distance versus the cracks size ratio. In this case the longer crack has a length ratio of $a/R=0.2$. (C) Normalized buckling load associated with the "M" and "N" -shaped interactional local buckling in cylinders with two crack of equal length, $a/R=0.2$ and different thickness, $t/R=0.003$, 0.006 and 0.01.

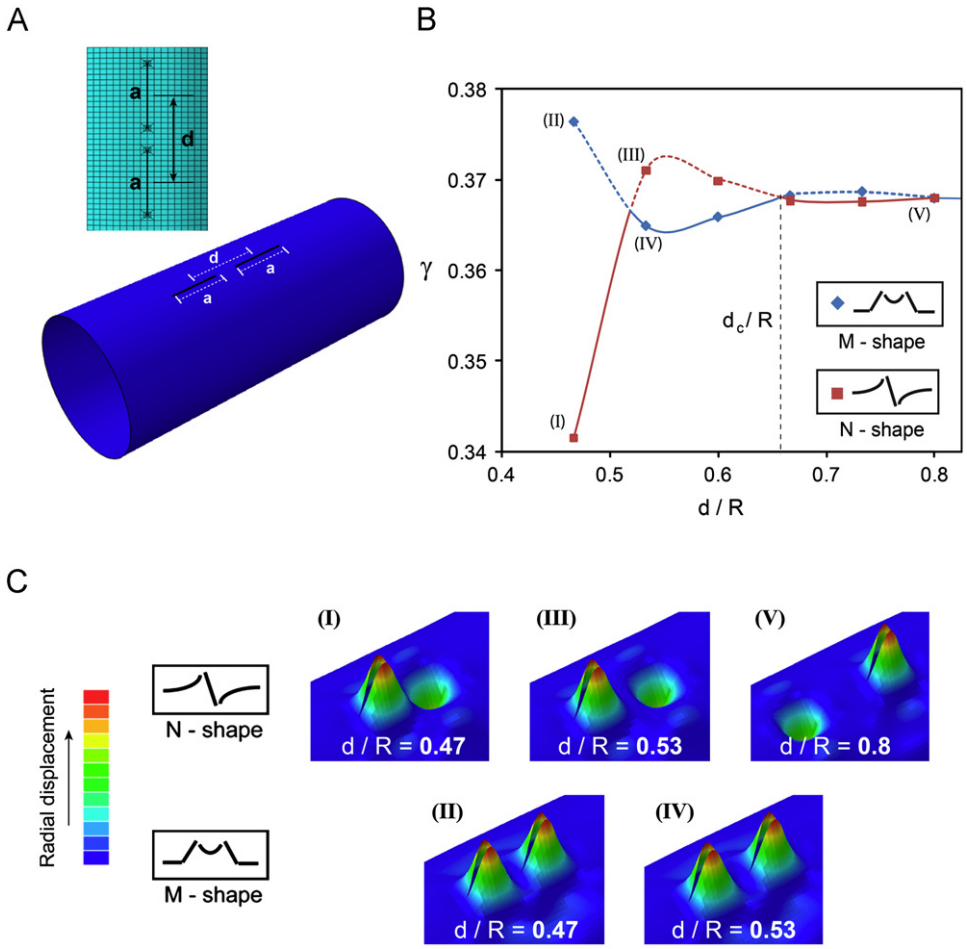

Fig. 9. Local buckling of a cylindrical shell with two equal-size vertically oriented collinear cracks. (A) Schematic of the cracked cylinder and the meshing scheme used for analysis. (B) Normalized buckling load versus the distance of the two cracks for a cylinder with $t/R=0.01$ and $a/R=0.2$. The solid line correspondes to the first buckling mode while the dashed line denotes the second mode of buckling. The red squares and blue diamonds correspond to the "M" and "N" shapes of buckling, respectively. (C) "N" and "M" shaped local buckling deformations for double-cracked cylinders of different crack distance, indicated in Fig. 9B. (For interpretation of the references to color in this figure legend, the reader is referred to the web version of this article.)

In Fig. 9, we repeated similar calculations for a double cracked cylindrical shell with two equal-size longitudinal collinear cracks. Analogously to the results presented in Fig. 7, two buckling shapes were identified which resemble the 'M-shape' and 'N-shape' modes discussed before. In this figure, d is again defined as the distance between the centers of the two cracks (thus, $d>a$ in order to have two separate cracks). In Fig. 9B, we plotted the buckling load associated with each of the above buckling shapes ('M' and 'N' shapes) for the cylinder with $t/R=0.01$, $a/R=0.2$ and different crack distances, d. For cylinders with $d/R<0.52$ or $0.66<d/R$, the N-shape buckling mode is the first buckling shape and for two cracks with $0.52<d/R<0.66$, the M shape of buckling becomes the first buckling mode. Also in this case, the normalized maximum interaction distance of $d/R\simeq 0.8$ was obtained, which is slightly larger than the maximum interaction distance of the counterpart cylinder (same thickness and crack size) with parallel offset cracks.

5. Cylindrical shells with multiple longitudinal cracks

Based on the maximum interaction distance d_{im} of adjacent longitudinal cracks, it seems reasonable that the behavior of many equally spaced cracks might also be understood based on that same distance – particularly, if the spacing is greater than d_{im}, the buckling load will be that of just one isolated crack of the same size. Fig. 10A shows the normalized buckling load versus the normalized thickness of cylindrical shell of thickness t and radius R, for three different crack configurations: (i) one longitudinal crack, (ii) two parallel longitudinal cracks of equal size located at distance $d=0.39R$, and (iii) multiple parallel longitudinal cracks (for a total of 16) at a fixed distance from each other, $d=0.39R$. The results are presented for fixed crack length, $a=0.2R$. For cylinders with many cracks and with a relatively thin shell (e.g. $t/R<0.0033$ at this crack length), the local buckling deformation at each crack opening is not influenced by the presence of other cracks. With this spacing, the buckling loads of cylinders with single, double, and multiple cracks are practically identical. By increasing the thickness of the shell ($t/R>0.0033$ in this set of calculations), d_{im} grows and the cracks begin to interact: the buckling deformation near each crack is influenced by its neighbor. As a result, cylindrical shells with a greater number of interacting cracks have lower buckling loads in the local interactive buckling regime. As the shell thickness further increases, the buckling of the shell becomes transitional and then global. In the latter case, the buckling load of the cylindrical shells for the three configurations is $\gamma\sim 1$. In Fig. 10B the local buckling shape for two thickness ratios of $t/R=0.002$ and 0.01 are shown for cylindrical shells with 1 and 16 cracks. At $t/R=0.002$ due to the lack of interaction between the cracks, there is nearly no difference in the local buckling deformation at the crack opening between the two cases. In this case, the buckling pattern at the cylindrical shell with 16 cracks has a 16-fold rotational symmetry. However, for the cylinder with $t/R=0.01$ the cracks interact in a way that favors anti-

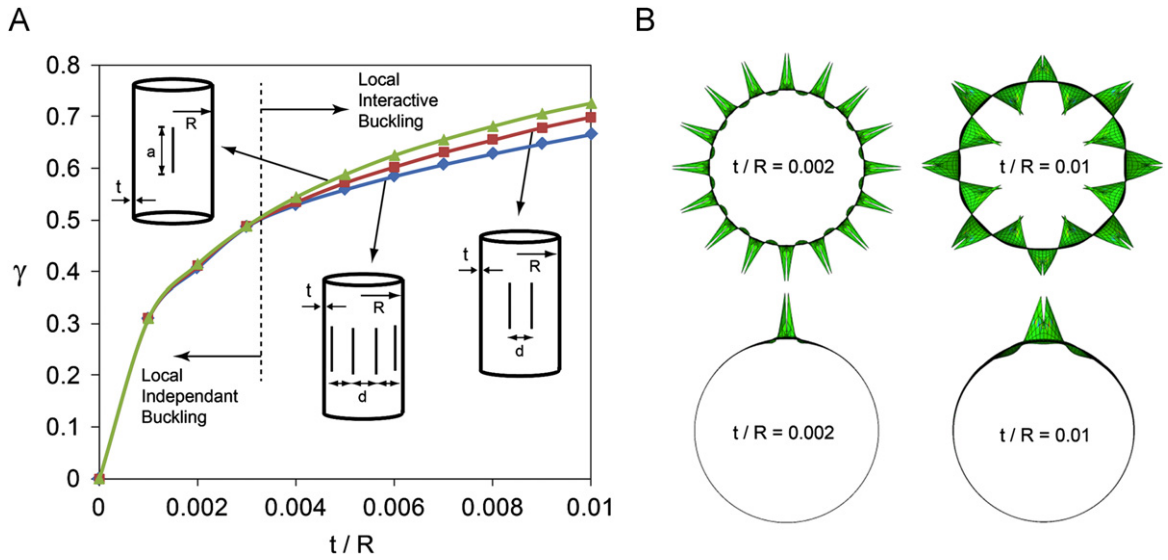

Fig. 10. (A) Normalized buckling load of a cylinder with single, double and multiple cracks of fixed distance, $d/R=0.39$, versus the shell thickness ratio. The crack size is fixed and equal to $a=0.2R$. (B) Local buckling modes corresponding to cylinders with 1 and 16 cracks and with the shell thickness ratios of $t/R=0.002$ and 0.01.

symmetric modes, resulting in only 8-fold rotational symmetry (this phenomenon requires an even number of cracks).

6. Post-buckling response of cracked shells

It should be noted that the eigenvalue analysis does not necessary predict the overall collapse of the cylinder. For example, in the case of cylinder with two parallel cracks, the eigenvalue analysis may obtain the eigenvalue that corresponds to the premature local buckling deformation of the curved strip between two cracks. This does not necessarily result in the overall collapse of the cylindrical shell [39]. To illustrate this, we carried out a preliminary post-buckling analysis of longitudinally cracked cylinders with a single crack using finite element analysis. The post-buckling response of the cracked shells was obtained by using a stabilizing mechanism based on automatic addition of volume-proportional damping [40,41]. For each set of calculations, the damping value was decreased systematically to assure that the response is insensitive to this change [40]. No initial geometric or material imperfection was included in the computational models. The post-buckling analysis showed that the force-strain response of an elastic cracked shell is almost linear before and after local buckling until the overall collapse of the structure. Fig. 11 shows the results of our preliminary study on the buckling of a cylindrical shell with a longitudinally oriented crack with $a/R=0.2$, using both eigenvalue and post-buckling analyses. In this figure the normalized buckling loads of the cracked cylinder is plotted as a function of the crack size ratio, a/R. In the case of a perfect cylinder the buckling load is almost equal to 1 and the buckling shape is global. For the a cracked cylindrical shell with $a/R<0.06$, the buckling deformation is axisymmetric and sinusoidal along the axial direction (global buckling). For values of $0.06<a/R<0.18$ the buckling deformation first occurs locally at the crack region but does not considerably affect the overall response of the cylinder. The collapse occurs at $\gamma=1$ accompanied by the axisymmetric sinusoidal wrinkling of the cylindrical shell (global buckling). In the range of $0.18<a/R<0.26$ the buckling first happens locally at the crack region and then the buckling deformations are increased until they cause the entire structure to collapse at the load ratio $\gamma<1$. For $a/R>0.26$ the eigenvalue and post-buckling load of the cylindrical shell coincide and the structure will collapse

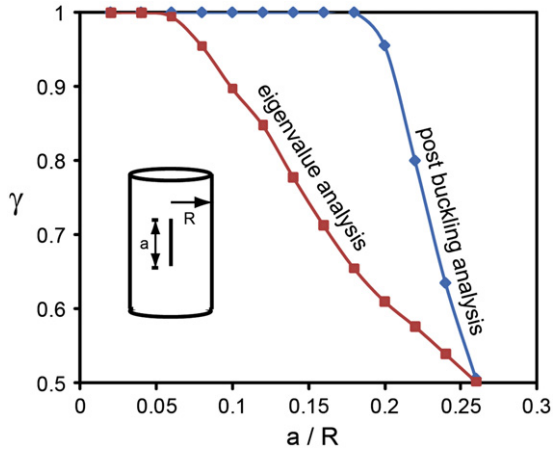

Fig. 11. Normalized buckling load versus crack size from post buckling (blue line) and eigen value (red line) analysis of the cracked cylinderical shell with $a/R=0.2$. The normalized shell thickness is $t/R=0.006$. (For interpretation of the references to color in this figure legend, the reader is referred to the web version of this article.)

as soon as the local buckling at the crack region occurs. Further post-buckling analysis is required to provide a complete understanding of the role of cracks on the overall collapse load of cracked shells.

7. Concluding remarks

We performed eigenvalue analysis to explore the linear buckling behavior of cylindrical shells with single or multiple cracks under axial-compression. For a cylinder with a single crack, a thorough parametric study on the effect of crack length and angle on the buckling load and shape of the cylinder has been carried out. The current investigation complements previous studies on the behavior of single cracked cylinders [16,19] and more specifically highlights the role of crack angle. Based on eigenvalue analysis, a longitudinal crack has the most detrimental effect on the buckling load of a single-cracked cylindrical shell. The local buckling shape mainly depends on the crack angle and is insensitive to the crack length and shell thickness.

For cylinders with two cracks, the buckling behavior is influenced not only by the buckling behavior of each individual crack but also by the interaction between the cracks. By increasing the separation between the two cracks above a particular separation distance called the maximum interaction distance, crack-interaction effects on the buckling load vanish. The maximum interaction distance in the two basic cases of two longitudinal cracks with co-centered (i.e., parallel offset) or collinear orientations was shown to decrease by reducing the size of the two cracks or the thickness of the shell. Finally, the case of a cylindrical shell with multiple cracks with and without interaction was studied. If the crack separation distances are all larger than the maximum interaction distance, then the buckling behavior is regulated by the largest crack. In this case, the buckling load of the cylinder is approximately equal to the buckling load of a counterpart single-cracked cylinder containing only the largest crack. The results provide insight into the buckling behavior of shells with defects and more specifically cracks.

Acknowledgment

The authors thank Dr. Jim Papadopoulos, Dr. Hamid Nayeb-Hashemi and Dr. John W. Hutchinson for fruitful discussions. This work was supported in part by the NSF CMMI grant award no. 1065759.

References

[1] Javidruzi M, Vafai A, Chen JF, Chilton JC. Vibration, buckling and dynamic stability of cracked cylindrical shells. Thin-Walled Structures 2004;42:79–99.
[2] Rajani B, Kleiner Y. Comprehensive review of structural deterioration of water mains: physically based models. Urban Water 2001;3:151–64.
[3] Makar JM, Desnoyers R, McDonald SE. Failure modes and mechanisms in gray cast iron pipe 2001:1–10.
[4] Rajani BB, Zhan C, Kuraoka S. Pipe-soil interaction analysis of jointed water mains. Canadian Geotechnical Journal 1996;33:393–404.
[5] Li YW, Elishakoff I, Starnes JH, Bushnell D. Effect of the thickness variation and initial imperfection on buckling of composite cylindrical shells: Asymptotic analysis and numerical results by BOSOR4 and PANDA2. International Journal of Solids and Structures 1997;34:3755–67.
[6] Anderson RB, Sullivan TL. Fracture Mechanics of Through-Cracked Cylindrical Pressure Vessels. In: NASA TN D-3252; 1966.
[7] Erdogan F, Kibler JJ. Cylindrical and spherical shells with cracks. International Journal of Fracture 1969;5:229–37.
[8] Copley LG, Sanders JL. A longitudinal crack in a cylindrical shell under internal pressure. International Journal of Fracture 1969;5:117–31.
[9] Erdogan F, Ratwani M. A circumferential crack in a cylindrical shell under torsion. International Journal of Fracture 1972;8:87–95.
[10] Duncan-Fama M, Sanders J. A circumferential crack in a cylindrical shell under tension. International Journal of Fracture 1972;8:15–20.
[11] Budiansky B, JW H. Contributions to the Theory of Aircraft Structures. In: Buckling of circular cylindrical shells under axial compression. Delft University Press, 1972, pp. 239–260.
[12] Xie YJ. A theory on cracked pipe. International Journal of Pressure Vessels and Piping 1998;75:865–9.
[13] Xie YJ. An analytical method on circumferential periodic cracked pipes and shells. International Journal of Solids and Structures 2000;37:5189–201.
[14] Hutchinson JW. Buckling and Initial Postbuckling Behavior of Oval Cylindrical Shells under Axial Compression. Journal of Applied Mechanics 1968;35:66–72.
[15] Hutchinson JW. On the Postbuckling Behavior of Imperfection-Sensitive Structures in the Plastic Range. Journal of Applied Mechanics 1972;39:155–62.
[16] Estekanchi HE, Vafai A. On the buckling of cylindrical shells with through cracks under axial load. Thin-Walled Structures 1999;35:255–74.
[17] Vafai A, Estekanchi HE. A parametric finite element study of cracked plates and shells. Thin-Walled Structures 1999;33:211–29.
[18] Vafai A, Javidruzi M, Estekanchi HE. Parametric instability of edge cracked plates. Thin-Walled Structures 2002;40:29–44.
[19] Vaziri A. On the buckling of cracked composite cylindrical shells under axial compression. Composite Structures 2007;80:152–8.
[20] Estekanchi HE, Vafai A, Kheradmandnia K. Finite element buckling analysis of cracked cylindrical shells under torsion. Asian Journal of Civil Engineering 2002;3:73–84.
[21] Vaziri A, Estekanchi HE. Buckling of cracked cylindrical thin shells under combined internal pressure and axial compression. Thin-Walled Structures 2006;44:141–51.
[22] Starnes JH, Rose CH. Nonlinear response of Thin Cylindrical Shells With Longitudinal Cracks and Subjected to Internal Pressure and Axial Compression Loads. In: NASA Langley Technical Report Server; 1997.
[23] Starnes JH, Rose CH. Buckling and Stable Tearing Responses of Unstiffened Aluminum Shells With Long Cracks. In: NASA Langley Technical Report Server; 1998.
[24] Hung ND, Ngoc TT. Analysis of cracked plates and shells using metis finite element model. Finite Elements in Analysis and Design 2004;40:855–78.
[25] Wyart E, Coulon D, Duflot M, Pardoen T, Remacle JF, Lani F. A substructured FE-shell/XFE-3D method for crack analysis in thin-walled structures. International Journal for Numerical Methods in Engineering 2007;72:757–79.
[26] Schenk CA, Schuëller GI. Buckling analysis of cylindrical shells with random geometric imperfections. International Journal of Non-Linear Mechanics 2003;38:1119–32.
[27] Brighenti R. Buckling of cracked thin-plates under tension or compression. Thin-Walled Structures 2005;43:209–24.
[28] Vaziri A, Nayeb-Hashemi H, Estekanchi HE. Buckling of the Composite Cracked Cylindrical Shells Subjected to Axial Load. ASME Conference Proceedings 2003;2003:87–93.
[29] Koiter WT. The effect of axisymmetric imperfections on the buckling of cylindrical shells under axial compression. Proceedings of the Koninklijke Nederlandse Akademie van Wetenschappen 1963.
[30] Weingarten VI, Morgan EJ, Seide P. Elastic stability of thin-walled cylindrical and conical shells under axial compression. AIAA 1965;3:500–6.
[31] Hutchinson JW. Buckling and Initial Postbuckling Behavior of Oval Cylindrical Shells under Axial Compression. Journal of Applied Mechanics 1968:66–72.
[32] Weingarten VI, Morgan EJ, Seide P. Elastic stability of thin-walled cylindrical and conical shells under cobmined external pressure and axial compression, 3. AIAA; 1965, pp. 913–20.
[33] Weingarten VI, Morgan EJ, Seide P. Elastic stability of thin-walled cylindrical and conical shells under cobmined external pressure and axial compression. AIAA 1965;3:1118–25.
[34] Foster C. Axial compression buckling of conical and cylindrical shells. Experimental Mechanics 1987;27:255–61.
[35] Krishnakumar S, Foster C. Axial load capacity of cylindrical shells with local geometric defects. Experimental Mechanics 1991;31:104–10.
[36] Hutchinson JW, Muggeridge DB, Tennyson RC. Effect of a local axisymmetric imperfection on the buckling behaviorof a circular cylindrical shell under axial compression. AIAA 1971;9:48–52.
[37] Hilburger MW, Starnes Jr JH. Effects of imperfections on the buckling response of compression-loaded composite shells. International Journal of Non-Linear Mechanics 2002;37:623–43.
[38] Timoshenko SP, Green JM. Theory of elastic stability. McGraw-Hill Book Co.; 1961.
[39] Shariati M, Sedighi M, Saemi J, Eipakchi HR, Allahbakhsh HR. Numerical and experimental investigation on ultimate strength of cracked cylindrical shells subjected to combined loading. Mechanika 2010;4:12–9.
[40] Vaziri A. Mechanics of highly deformed elastic shells. Thin-Walled Structures 2009;47:692–700.
[41] Cao Y, Hutchinson JW. From wrinkles to creases in elastomers: the instability and imperfection-sensitivity of wrinkling. In: Proceedings of the Royal Society A: Mathematical, Physical and Engineering Science; 2011.